

# New RP-CVD grown ultra-high performance selectively B-doped pure-Ge 20 nm QWs on (100)Si as basis material for post-Si CMOS technology

O. A. Mironov<sup>\*1,2</sup>, A. H. A. Hassan<sup>1,3</sup>, M. Uhlarz<sup>4</sup>, S. Kiatgamolchai<sup>5</sup>, A. Dobbie<sup>1</sup>, R. J. H. Morris<sup>1</sup>, J. E. Halpin<sup>1</sup>, S. D. Rhead<sup>1</sup>, P. Allred<sup>1</sup>, M. Myronov<sup>1</sup>, S. Gabani<sup>6</sup>, I. B. Berkutov<sup>7</sup>, and D. R. Leadley<sup>1</sup>

<sup>1</sup> Department of Physics, University of Warwick, Coventry, CV4 7AL, UK

<sup>2</sup> International Laboratory of High Magnetic Fields and Low Temperatures, 53-421 Wroclaw, Poland

<sup>3</sup> Department of Physics, Tripoli University, Tripoli, Libya

<sup>4</sup> Dresden High Magnetic Field Laboratory (HLD), HZDR, Dresden, Germany

<sup>5</sup> Department of Physics, Chulalongkorn University, Patumwan, Bangkok 10330, Thailand

<sup>6</sup> Centre of Low Temperature Physics, Institute of Experimental Physics SAS, Kosice, Slovakia

<sup>7</sup> B.I. Verkin Institute for Low Temperature Physics and Engineering of NAS of Ukraine, Kharkov, Ukraine

Received 24 May 2013, accepted 1 November 2013

Published online 10 December 2013

**Keywords** pure strained Ge channel, ultra-high mobility, SdH oscillation, impurity scattering

\* Corresponding author: e-mail oamironov@yahoo.co.uk, O.A.Mironov@warwick.ac.uk, Phone: +44 2476522448, Fax: +44 76692016

Magnetotransport studies at low and room temperature are presented for two-dimensional hole gases (2DHG) formed in fully strained germanium (sGe) quantum wells (QW). Two designs of modulation doped heterostructure grown by reduced pressure chemical vapour deposition (RP-CVD) were used and included a normal structure (doping above the Ge channel and inverted structure (doping beneath the Ge channel). The mobility ( $\mu_H$ ) for the normal structure was measured to be  $1.34 \times 10^6 \text{ cm}^2/\text{Vs}$  with a sheet density ( $p_s$ ) of  $2.9 \times 10^{11} \text{ cm}^{-2}$  at 1.5 K, and  $\mu_H = 3970 \text{ cm}^2/\text{Vs}$  and  $p_s \sim 1 \times 10^{11} \text{ cm}^{-2}$  for room temperature, determined from simulation using the Maximum Entropy- Mobility Spectrum Analysis (ME-MSA) method.

For the inverted structure a  $\mu_H$  of  $4.96 \times 10^5 \text{ cm}^2/\text{Vs}$  and  $p_s$  of  $5.25 \times 10^{11} \text{ cm}^{-2}$  was measured at 90 mK. From the temperature dependent amplitude of Shubnikov de Haas oscillations, the normal structure was found to have a very low effective mass ( $m^*$ ) value of  $0.063 m_0$  and a ratio of transport to quantum lifetime ( $\alpha$ ) of  $\sim 78$ . This extremely high  $\alpha$  is indicative of the carrier transport being dominated by small angle scattering from remote impurities i.e. a sample having an extremely low background impurity level and very smooth hetero-interfaces. The inverted structure had an  $m^*$  of  $0.069 m_0$  and  $\alpha \sim 29$ , which also indicates exceedingly high quality material.

© 2013 WILEY-VCH Verlag GmbH & Co. KGaA, Weinheim

**1 Introduction** One of the most important results of applying strain to Ge is to induce a reduction of the effective mass which directly impacts on the carrier mobility [1]. For that reason compressive strained germanium heterostructures have been studied in search of creating higher hole mobilities. A hole mobility of up to  $10^6 \text{ cm}^2/\text{Vs}$  at a sheet density  $3 \times 10^{11} \text{ cm}^{-2}$  was reported for a “normal” heterostructure design i.e. with the doping above the channel [2] and is the highest hole mobility at 12 K currently in the literature [2-6]. However, the room temperature (RT) mobility becomes the most important

mobility for device applications. The problem with trying to measure the RT mobility in modulation doped heterostructures is the numerous parallel conduction layers i.e. all the layers contribute to the measured mobility at RT. A theoretical approach, previously described as Maximum Entropy-Mobility Spectrum Analysis (ME-MSA) [7], has been applied to the experimental data in order to obtain the individual layer’s carrier conductivity, mobility and sheet densities at (RT). The technique exploits the magneto-transport data over a range of magnetic fields in order to extract the RT mobility. From the ME-MSA results the

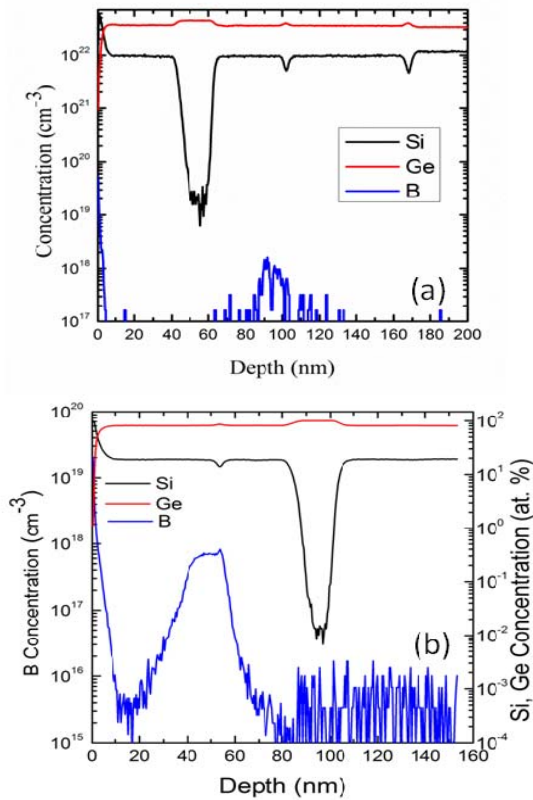


**Figure 1** SIMS depth profile for Si, Ge and B from (a) the inverted structure (11-284) using an  $O_2^+$  primary beam and (b) the normal structure (11-289) using a Cs primary ion beam.

highest RT hole mobility to date of  $3970 \text{ cm}^2/\text{V}\cdot\text{s}$  at  $p_s \sim 9.76 \times 10^{10} \text{ cm}^{-2}$  was found compared to current literature [8-13].

In this paper, we present the electrical characterization of a high purity sGe channel grown on top of a  $\text{Si}_{0.2}\text{Ge}_{0.8}$  layer by analyzing the Shubnikov de Haas (SdH) oscillations from magnetotransport measurements to calculate the mobility at RT and low temperature (0.09-1.5 K, inverted structure, and 1.5-4 K normal structure) from which parameters including the effective mass ( $m^*$ ) and the Dingle ratio of transport to quantum lifetime ( $\alpha$ ) were ascertained. This study also shows the highest  $\alpha$  and lowest  $m^*$  found for a fully strained Ge 2DHG.

## 2 Experimental results

**2.1 Sample design and fabrication** Both inverted (doping below channel) and normal (doping above channel) type sGe heterostructures were for this study grown using an ASM Epsilon 2000 reduced pressure chemical vapour deposition (RP-CVD) chamber. The structures contain a  $20 \pm 1 \text{ nm}$  fully strained germanium channel on a strain relaxed buffer [15], which was grown at  $400 \text{ }^\circ\text{C}$  without any chemical mechanical polishing (CMP) and has a low threading dislocation density (TDD) of  $\leq 4 \times 10^6 \text{ cm}^{-2}$  [16, 17]. Both heterostructures were

analysed by ultra-low energy SIMS (uleSIMS) depth profiles using a near normal incidence  $O_2^+$  primary beam at  $250 \text{ eV}$  [14], while the normal heterostructure was also investigated using Cs at a higher energy (Fig. 1). The uleSIMS measurements show that the doping layer in the normal structure is  $13 \text{ nm}$  thick, with an average B-density of  $1.4 \times 10^{18} \text{ cm}^{-3}$  located above a  $26 \pm 1 \text{ nm}$  thick spacer. For the inverted structure, the doping layer (underneath the channel) was  $18 \pm 2 \text{ nm}$  thick with an average B concentration of  $7 \times 10^{17} \text{ cm}^{-3}$ . These SIMS profiles also confirm the purity of Ge channel, with less than 0.01% Si.

Transport measurements from RT down to 10 K were performed using  $4 \times 4 \text{ mm}^2$  square VdP samples. For the low temperature measurements, Hall bar devices were fabricated on both the inverted and normal heterostructures, with a width  $50 \text{ }\mu\text{m}$  and probe arm separations of either  $250 \text{ }\mu\text{m}$  or  $500 \text{ }\mu\text{m}$ . The fabrication process used wet etching while Al contacts were deposited by thermal evaporation and annealed at  $425 \text{ }^\circ\text{C}$  for 20 min under dry  $N_2$  to enable an Al-Si eutectic needle-like

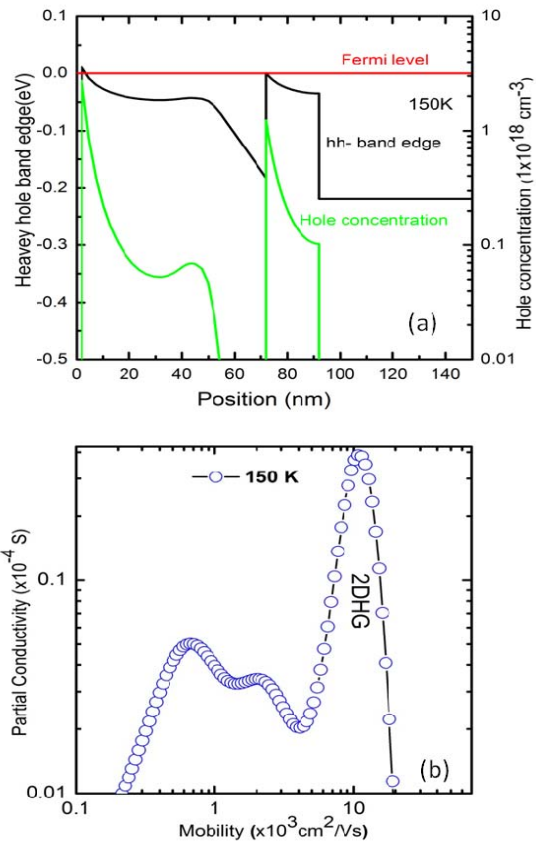


**Figure 2** (a) Next nano simulation for heavy hole band edge and sheet density at 150 K. (b) ME-MSA simulation for mobility, conductivity and sheet density at 150 K.

penetration to a depth of 60-120 nm and establish an ohmic contact to the Ge-QW.

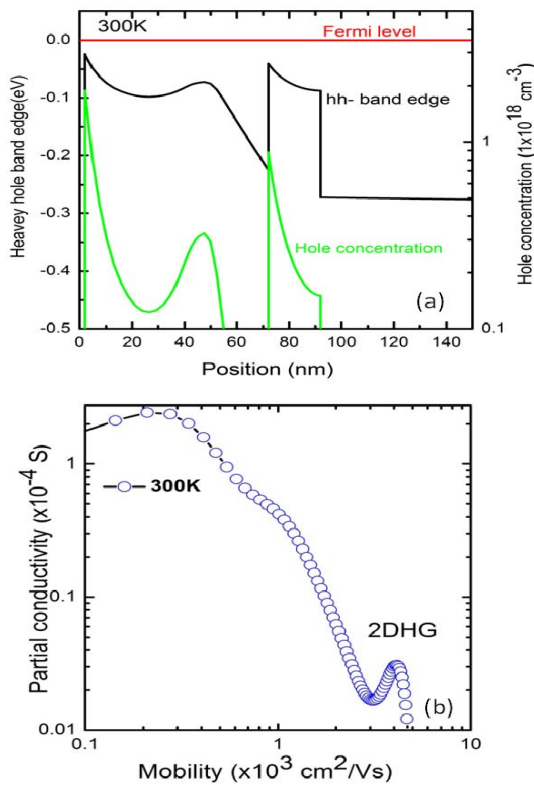


**Figure 3** (a) Band edge and sheet density simulation at 300 K for normal configuration, (b) ME-MSA simulation for normal structure (11-289-SQ1) at 300 K.

| T (K) | Nextnano <sup>3</sup> [18]             | ME-MSA                                 |                                      |
|-------|--|--|--------------------------------------|
|       | $p_s$<br>( $10^{11} \text{ cm}^{-2}$ ) | $p_s$<br>( $10^{11} \text{ cm}^{-2}$ ) | $\mu$<br>( $\text{cm}^2/\text{Vs}$ ) |
| 150   | 1.79                                   | 2.37                                   | 10660                                |
| 300   | 1.41                                   | 0.98                                   | 3970                                 |

**Table 1** Result of the simulation of normal configuration by Nextnano program and ME-MSA method.

**2.2 Magnetotransport results at 300 K-10 K and ME-MSA analysis** Magnetotransport measurements were performed using the Van der Pauw configuration [1, 17]. The measured RT hole mobility was  $1063 \text{ cm}^2/\text{Vs}$  at a  $p_s = 2.23 \times 10^{13} \text{ cm}^{-2}$ . Using ME-MSA [7] we extracted the 2DHG channel mobility and sheet density over the temperature range 50 to 300 K. The calculated mobility by ME-MSA at 150 K and 300 K are shown in Fig. 2b and 3b, as well as the simulation of the band edge and heavy hole concentration using effective mass approximation to solve Schrödinger Poisson equation in Nextnano<sup>3</sup> program [18] at the same temperature. Table 1 summarizes the results for both methods, whereby three hole mobility peaks are clearly visible for this structure. These peaks represent the hole concentration within the various layers which include the 2DHG Ge channel, the B supply layer and the holes in

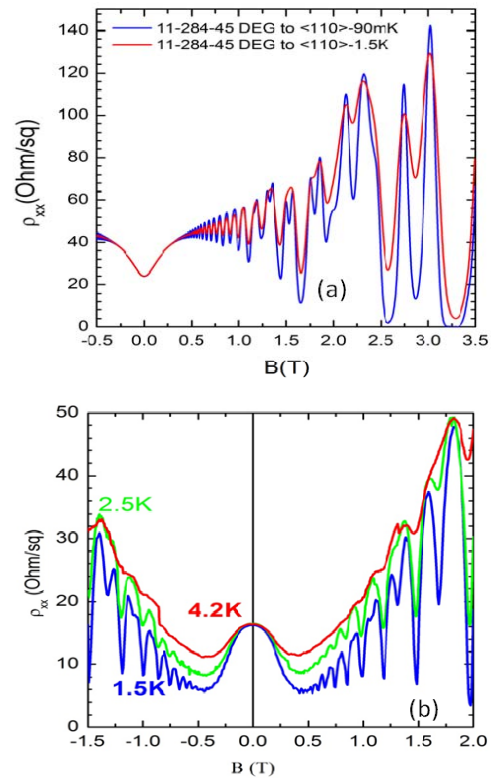


**Figure 4** (a) SdH oscillation for inverted configuration 11-284 at two orientation 45DEG and 90 DEG at 250 mK. (b) SdH oscillation for normal configuration 11-289-90DEG

Si cap, where B is clearly observed within the SIMS profiles.

**2.3 Low-temperature transport results** The hole mobility and carrier sheet density for the samples were determined using standard resistivity and Hall measurements at temperatures down to 12 K. The result at 12 K for the normal structure (previously published [1, 19]) showed a mobility of  $1.1 \times 10^6 \text{ cm}^2/\text{Vs}$  at a carrier sheet density of  $3.0 \times 10^{11} \text{ cm}^{-2}$ . The inverted structure [18] had mobility of  $0.255 \times 10^6 \text{ cm}^2/\text{Vs}$  at  $p_s = 6.3 \times 10^{11} \text{ cm}^{-2}$ . These significant results motivated the further study of these samples.

Magnetotransport measurement of  $\rho_{xx}$  and  $\rho_{xy}$  were made over temperatures of 500 mK - 4.2 K for sample 11-289 (normal structure) and 90 mK - 1.5 K for 11-284 (inverted) (Fig. 4a and 4b). An extremely high mobility of  $1.34 \times 10^6 \text{ cm}^2/\text{Vs}$  at  $p_s = 2.9 \times 10^{11} \text{ cm}^{-2}$  has been determined for the normal heterostructure at 500 mK. This result for holes in germanium is comparable with the highest reported electron mobility for a 2DEG stretched silicon channel of  $1.6 \times 10^6 \text{ cm}^2/\text{Vs}$  at a carrier sheet density of  $1.5 \times 10^{11} \text{ cm}^{-2}$  observed at 0.3 K [20]. The mobility for the inverted structure was found to be  $0.51 \times 10^6 \text{ cm}^2/\text{Vs}$  at  $p_s = 5.1 \times 10^{11} \text{ cm}^{-2}$  at 90 mK, which also exceeds all previous results for holes in compressively strained Ge

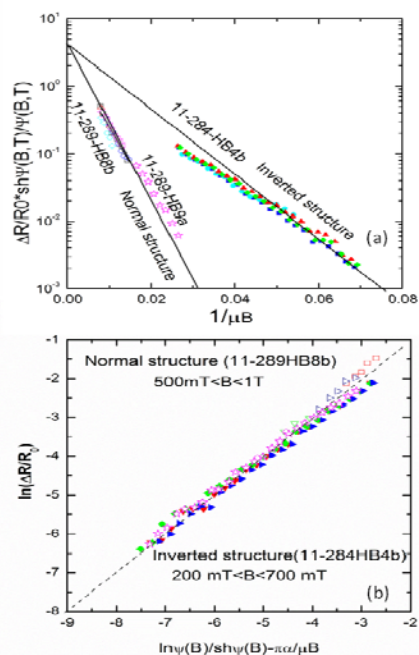


**Figure 5** (a) Dingle plot for normal and inverted structures. (b) Plot to obtain effective mass for both inverted and normal structures.

apart from our normal structure. To calculate  $m^*$ , the amplitude of the Shubnikov de Haas oscillations were measured over a range of different temperatures and magnetic fields [8]. The normal structure was found to have the lowest value of hole  $m^*$  published to date ( $0.063 \pm 0.001 m_0$ ) (Fig. 3c), while the inverted structure  $m^*$  was found to be  $0.069 \pm 0.002 m_0$ . This extremely low  $m^*$  will have a significant contribution to the vastly improved mobility observed. The Dingle plot in Fig. 5a illustrates a straight line intercept with the Y-axis at “4” which is in excellent agreement with the theory [21], and relates to homogeneous broadening of the Landau levels. The  $\alpha$  was found from the slope of Fig. 5a to be  $78 \pm 2$  for the normal structure and  $29 \pm 2$  for the inverted structure. This value of  $\alpha$  indicates that the mobility in both structures is limited by small angle scattering for remote impurities with no effect of background impurities in the Ge channel [22].

**Acknowledgements** This work has been partially supported by the EPSRC UK *Renaissance Germanium* project EP/F031408 and the grant of the Slovak Research and Development Agency under the contract No. APVV-0132-11, VEGA-0106-13, and SAS Centre of Excellence CFNT MVEP. OAM acknowledged National Scholarship Program of the Slovak Republic for the Mobility Support for Researchers in the Academic Year 2012/2013.

## References

- [1] K. Sawano, K. Toyama, R. Masutomi, T. Okamoto, N. Usami, K. Arimoto, K. Nakagawa, and Y. Shiraki, *Appl. Phys. Lett.* **95**(12), 3 (2009).
- [2] A. Dobbie, M. Myronov, R. J. H. Morris, A. H. A. Hassan, M. J. Prest, V. A. Shah, E. H. C. Parker, T. E. Whall, and D. R. Leadley, *Appl. Phys. Lett.* **101**(17), 172108 (2012).
- [3] S. Madhavi, V. Venkataraman, and Y. H. Xie, *Appl. Phys. Lett.* **89**, 2497 (2001).
- [4] M. Myronov, T. Irisawa, S. Koh, O. A. Mironov, T. E. Whall, E. H. C. Parker, and Y. Shiraki, *J. Appl. Phys.* **97**(8) (2005).
- [5] B. Rossner, D. Chrastina, G. Isella, and H. von Kanel, *Appl. Phys. Lett.* **84**(16), 3058-3060 (2004).
- [6] T. Irisawa, M. Myronov, O. A. Mironov, E. H. C. Parker, K. Nakagawa, M. Murata, S. Koh, and Y. Shiraki, *Appl. Phys. Lett.* **82**(9), 1425-1427 (2003).
- [7] H. von Kanel, M. Kummer, G. Isella, E. Muller, and T. Hackbarth, *Appl. Phys. Lett.* **80**(16), 2922-2924 (2002).
- [8] S. Kiatgamolchai, M. Myronov, O. A. Mironov, V. G. Kantser, E. H. C. Parker, and A. T. E. Whall, *Phys. Rev. E* **66**, 036705 (2002).
- [9] T. Tanaka, Y. Hoshi, K. Sawano, N. Usami, Y. Shiraki, and K. M. Itoh, *Appl. Phys. Lett.* **100**, 222102 (2012).
- [10] T. Irisawa, H. Miura, T. Ueno, and Y. Shiraki, *Jpn. J. Appl. Phys., Part 1* **40**(4B), 2694-2696 (2001).
- [11] R. J. H. Morris, T. J. Grasby, R. Hammond, M. Myronov, O. A. Mironov, D. R. Leadley, T. E. Whall, E. H. C. Parker, M. T. Currie, C. W. Leitz, and E. A. Fitzgerald, *Semicond. Sci. Technol.* **19**(10), L106-L109 (2004).
- [12] M. Myronov, T. Irisawa, O. A. Mironov, S. Koh, Y. Shiraki, T. E. Whall, and E. H. C. Parker, *Appl. Phys. Lett.* **80**(17), 3117-3119 (2002).
- [13] H. von Kanel, D. Chrastina, B. Rossner, G. Isella, J. P. Hague, and M. Bollani, *Microelectron. Eng.* **76**(1-4), 279-284 (2004).
- [14] R. J. H. Morris, M. G. Dowsett, R. Beanland, A. Dobbie, M. Myronov, and D. R. Leadley, *Analyt. Chem.* **84**(5), 2292-2298 (2012).
- [15] M. Myronov, A. Dobbie, V. A. Shah, X. C. Liu, V. H. Nguyen, and D. R. Leadley, *Electrochem. Solid State Lett.* **13**(11), H388-H390 (2010).
- [16] V. A. Shah, A. Dobbie, M. Myronov, D. J. F. Fulgoni, L. J. Nash, and D. R. Leadley, *Appl. Phys. Lett.* **93**(19) (2008).
- [17] V. A. Shah, A. Dobbie, M. Myronov, and D. R. Leadley, *J. Appl. Phys.* **107**(6), 064304 (2010).
- [18] <http://www.nextnano.de/nextnano3/>
- [19] A. Dobbie, M. Myronov, R. J. H. Morris, M. J. Prest, J. S. Richardson-Bullock, A. H. A. H. Hassan, V. A. Shah, E. H. C. Parker, T. E. Whall, and D. R. Leadley, *ISTDM 2012*, June 4-6, 2012, Berkeley, CA, USA.
- [20] R. R. Lieten, S. Degroote, M. Leys, N. E. Posthuma, and G. Borghs, *Appl. Phys. Lett.* **94**(11), 3 (2009).
- [21] A. Ishihara and L. Smrcka, *J. Phys. C* **19**(34), 6777 (1986).
- [22] A. Gold, *Phys. Rev. B* **35**(2), 723-733 (1987).